Analytical and Bioanalytical Chemistry
https://doi.org/10.1007/s00216-019-02276-1

RESEARCH PAPER

# Simultaneous evaluation of multiple microarray surface chemistries through real-time interferometric imaging

Elisa Chiodi[1,2] · Laura Sola[1] · Dario Brambilla[1] · Marina Cretich[1] · Allison Marie Marn[2] · M. Selim Ünlü[2] · Marcella Chiari[1]

Received: 5 September 2019 / Revised: 9 October 2019 / Accepted: 11 November 2019
© Springer-Verlag GmbH Germany, part of Springer Nature 2020

## Abstract

Surface chemistry is a crucial aspect for microarray modality biosensor development. The immobilization capability of the functionalized surface is indeed a limiting factor for the final yield of the binding reaction. In this work, we were able to simultaneously compare the functionality of protein ligands that were locally immobilized on different polymers, while on the same solid support, therefore demonstrating a new way of multiplexing. Our goal was to investigate, in a single experiment, both the immobilization efficiency of a group of reactive polymers and the resulting affinity of the tethered molecules. This idea was demonstrated by spotting many reactive polymers on a $Si/SiO_2$ chip and depositing the molecular probes on the spots immediately after. As a proof of concept, we focused on which polymers would better immobilize a model protein (α-Lactalbumin) and a peptide (LAC-1). We successfully showed that this protocol is applicable to proteins and peptides with a good efficiency. By means of real-time binding measurements performed with the interferometric reflectance imaging sensor (IRIS), local functionalization proved to be comparable to the classical flat coating solution. The final outcome highlights the multiplexing power of this method: first, it allows to characterize dozens of polymers at once. Secondly, it removes the limitation, related to coated surfaces, that only molecules with the same functional groups can be tethered to the same solid support. By applying this protocol, many types of molecules can be studied simultaneously and immobilization for each probe can be individually optimized.

**Keywords** IRIS · Interferometric reflectance imaging sensor · Functional polymers · Localized surface functionalization · Microarray · Binding kinetics

## Introduction

Microarrays are analytical devices that work by allowing specific binding between target probes immobilized on the surface (namely, spots) and analyte molecules in solution [1]. Since microarray-based assays were first introduced in 1995 [2], they have rapidly gained popularity in various biological research areas, due to their multiplexing capability and small volume requirement.

The effectiveness of a microarray-based experiment mostly depends on how the probe molecules are immobilized on the surface. As a matter of fact, the chosen immobilization method influences the stability of the molecules as well as their reactivity. For example, if the ligand is not stably bound, it may be lost throughout the experiment. On the contrary, if the probe is immobilized too tightly, it may be less flexible or lose its structure, and therefore have less sites available for binding.

Coating the slide surface with a hydrophilic polymer prior to spotting allows to create a uniform, homogeneous, thin, reactive layer on which the molecules can be immobilized as far from the surface as necessary for them to remain active.

Published in the topical collection *Advances in Direct Optical Detection* with guest editors Antje J. Baeumner, Günter Gauglitz and Jiri Homola.

**Electronic supplementary material** The online version of this article (https://doi.org/10.1007/s00216-019-02276-1) contains supplementary material, which is available to authorized users.

✉ Elisa Chiodi
elich@bu.edu

[1] Consiglio Nazionale delle Ricerche, Istituto di Scienze e Tecnologie Chimiche "Giulio Natta" (SCITEC), Via Mario Bianco 9, 20131 Milan, Italy

[2] Department of Electrical Engineering, Boston University, Photonics Center, 8, St. Mary's Street, Boston, MA 02215, USA

Published online: 04 January 2020

In the last 10 years, our group has introduced a family of *N*,*N*-dimethylacrylamide (DMA)-based polymers that form a thin film on different materials by a combination of physi- and chemisorption [3]. In an effort to tailor surface properties, the precursor of this polymer family, a copolymer of dimethylacrylamide with *N*-acryloyloxysuccinimide (NAS) and 3-(trimethoxysilyl)propyl methacrylate (MAPS), has been modified with several building blocks to introduce, for example, azide, alkyne, dibenzocyclooctine, maleimide, functionalities thanks to the reactivity of NAS with amino groups [4]. The introduction of other functional groups by post-polymerization modification (PPM) reactions and the combination of different monomers during the synthesis has allowed to generate many polymers, ten of which were used in this work (see Fig. 1 and Table 1 for monomer mole percent). All these polymers share a common backbone of DMA and MAPS which confers them adhesive properties on a variety of surfaces.

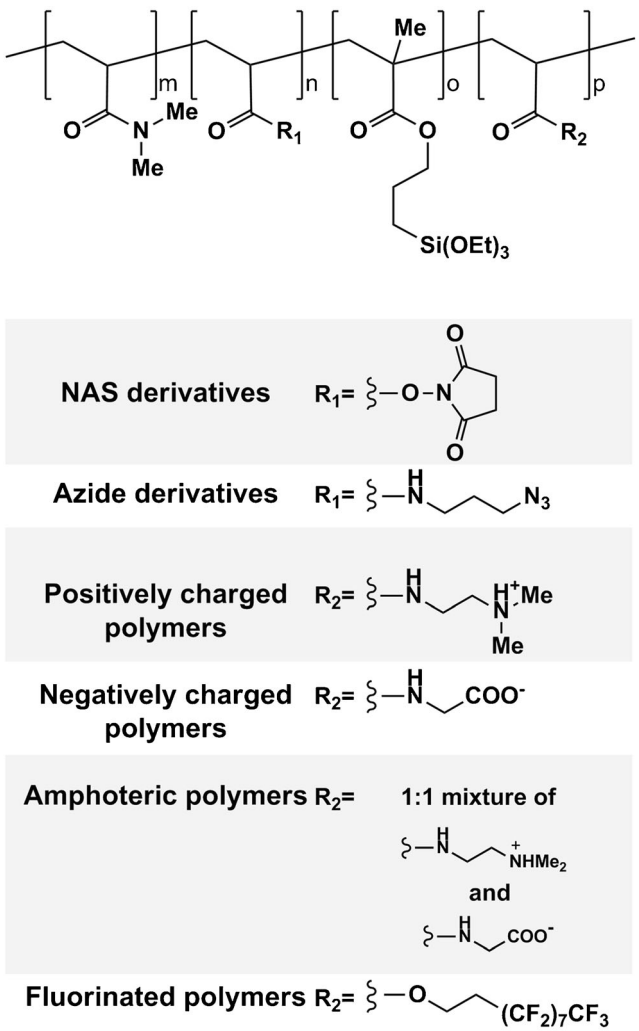


**Fig. 1** Chemical structure of tested copolymers, see Table 1 for monomer mole percentages

**Table 1** Mole percent of monomers used to synthesize polymers

| Copolymer | Monomer mole percent | | | |
|---|---|---|---|---|
| | m | n | o | p |
| Copoly NAS 10% | 89 | 10 | 1 | – |
| Copoly NAS 10% positive | 87 | 10 | 1 | 2 |
| Copoly NAS 10% negative | 87 | 10 | 1 | 2 |
| Copoly NAS 10% amphoteric | 87.5 | 10 | 0.5 | 2 |
| Copoly fluoride | 94 | 2 | 1 | 3 |
| Copoly azide | 97 | 2 | 1 | – |
| Copoly azide 10% | 89 | 10 | 1 | – |
| Copoly azide 10% negative | 87 | 10 | 1 | 2 |
| Copoly azide 10% amphoteric | 87.5 | 10 | 0.5 | 2 |
| Copoly azide fluoride | 94 | 2 | 1 | 3 |

The classical dip and rinse coating approach used with these polymers requires immersing the substrate in their aqueous solution followed by rinse and dry steps [5]. Thanks to the adhesive properties of the polymers, this approach, that is considerably simpler than most of the approaches used to produce polymeric coatings, was further simplified by localizing the coating through the spotting of only an ultra-small amount of polymer. Theoretically, dozens of different polymers could be arrayed on the surface, thus creating a number of different interfaces between the surface and the probes. Considering how many polymers are available and how differently they react with each probe, deciding which surface chemistry is the optimal one for every experiment is time consuming and laborious, as well as expensive. Indeed, the classical method would include coating many different slides with the different polymers one is willing to test, spotting each of them and performing measurements on them separately. This process results in a copious use of reagents, is time-consuming, and may also cause a non-trivial amount of statistical noise due to the experimental conditions that inevitably change for every experiment—for example, subtle changes in the temperature or in the pH of the solutions.

In this work, we combine the new approach for the immobilization of biomolecules based on spotting pL amounts of aqueous solutions of the various copolymers, followed by the deposition, on the same spot, of the biomolecule to be immobilized [6] with a real-time binding detection method [7] recently introduced by our group. This strategy provides an easy, inexpensive, and quick assay to test the influence of surface properties on binding affinity in tiny areas on which each probe is anchored on a chemically different environment in a single 60-min experiment.

## Material and methods

### Materials

*N*,*N*-Dimethylacrylamide (DMA), 3-(trimethoxylsilyl)propyl methacrylate (MAPS), 1H,1H,2H,2H-perfluorodecyl acrylate (PFDA), α,α′-azoisobutyronitrile (AIBN), acrylamido buffer pKa 3.6, acrylamido buffer pKa 8.5, dibenzocyclooctyne-*N*-hydroxysuccinimidyl ester (DBCO-NHS ester), anhydrous tetrahydrofuran (THF), petroleum ether, dimethylsulfoxide (DMSO), ammonium sulphate ($(NH_4)_2SO_4$), phosphate-buffered saline (PBS), sucrose monolaurate, Amicon Ultra centrifugal filters (MWCO 3K), and α-Lactalbumin were purchased from Sigma-Aldrich (St. Louis, MO, USA). Anti-α-Lactalbumin antibody was purchased from Abcam (Cambridge, UK). All solvents were used as received. *N*-Acryloyloxysuccinimide (NAS) and 3-azido-1-propylamine were synthesized as reported elsewhere [8, 9].

Untreated silicon slides with 110 nm thermally grown oxide were supplied by Silicon Valley Microelectronics (Santa Clara, CA, USA).

Spotting was performed using a SciFLEXARRAYER S12 (Scienion, Berlin, Germany).

### Polymer synthesis

All polymers, schematically represented in Fig. 1, were synthesized as previously reported [4, 10, 11]. Briefly, a 20% *w*/*v* total monomer concentration solution was prepared by dissolving each monomer (following the molar ratios reported in Table 1) in anhydrous THF. The solution was degassed for 20 min by purging argon into the monomer solution and then 2 mM of a thermoinitiator (AIBN) was added. The solution was heated for 2 h at 65 °C and kept under argon atmosphere. The solution was then diluted 1:1 with anhydrous THF and precipitated in petroleum ether (10 times the volume of the reaction mixture). Polymers were collected as a white powder and dried under vacuum at room temperature.

Polymers containing charged groups were synthesized using acrylamido derivatives with carboxyl or tertiary amino side chains. These monomers are commercially available under the trade name of acrylamido buffer. The pKa of their ionizable groups covers the entire pH scale. The acrylamido buffer with pKa 3.6 was used for the negative polymer, while the one with pKa 8.5 was chosen for the positive polymer. To synthesize the amphoteric polymer, a mixture of these acrylamido buffers was used.

Azide functionalities were introduced in parent polymers containing *N*-acryloyloxysuccinimide (NAS) via post-polymerization modification, as described elsewhere [4]. Essentially, the copolymer was dissolved in anhydrous THF to a final concentration of 20% *w*/*v*; a 2.5 M excess, with respect to the molar ratio of NAS, of 3-azido-1-propylamine was added to the crude material. The mixture was stirred for 5 h at room temperature under argon atmosphere and then diluted 1:1 with anhydrous THF. The polymers were precipitated in petroleum ether (10 times the volume of the reaction mixture), filtered on a Buchner funnel and dried under vacuum at room temperature.

### Synthesis of DBCO-modified α-Lactalbumin

3.53 μL of 40 mM solution of DBCO-NHS ester in DMSO (10 equivalents) was added to 100 μL of 1 mg/mL α-Lactalbumin in PBS and allowed to react for 30 min at room temperature. At the end, 10 μL of TRIS-HCl 1 M pH 8 was added to quench the reaction. After 5 min of quenching, the reaction mixture was filtered on Amicon Ultra 3 K centrifugal filter for 2 min at 12,000×*g* to remove unreacted DBCO-NHS ester. PBS was finally added to the DBCO-modified α-Lactalbumin solution to a final volume of 100 μL, and the solution was deposited on silicon slides without further purification.

### Synthesis of LAC-1 peptides

LAC-1 peptides synthesis is described elsewhere [12]. Sequences are reported in Table S1 (see Electronic Supplementary Material, ESM). Briefly, the peptides were assembled on a 2-CTC resin by a microwave-assisted Fmoc (fluorenylmethyloxycarbonyl protecting group) solid-phase peptide synthesis (SPPS) protocol, on a Biotage ALSTRA Initiator + Peptide synthesizer. Chain elongation was performed by iterative amino acids coupling cycles and Fmoc deprotection. Peptides were then cleaved from the resin and purified by RP-HPLC.

### IRIS system

The interferometric reflectance imaging sensor (IRIS) uses optical phase difference to detect very small amounts of biomass that accumulate on an active surface (ESM Fig. S1). The measurement concept and the setup were fully described in ref. [7, 13]. Briefly, the active surface is composed of a silicon chip with a thermally grown $SiO_2$ layer on top.

The chip contains two holes through the Si substrate to allow the passage of liquid across the active surface to conduct dynamic binding measurements. The layered sensor structure creates a common path interferometer where the reflectance at a particular wavelength depends directly on the thickness of the top transparent layer. In our system, the sample can be illuminated by four independent LEDs with a peak at four different visible wavelengths (455 nm, 518 nm, 598 nm, and 635 nm). By measuring the reflectance from the substrate at distinct wavelengths across the visible spectrum, we are able to reconstruct the reflectance curve from the layered substrate and deduce the thickness of the transparent layer with *pm* accuracy. Changes in the optical path length due to the capture of a target

of interest on the $SiO_2$ layer cause a measurable shift in this reflectance curve, and we are able to achieve *pg/mm²* sensitivity to target binding [7]. However, continuously acquiring images with each of these four illumination wavelengths throughout the experiment, and then calculating the reflectance curve for each four-color acquisition has practical limitations. Therefore, we start from the assumption that during the whole experiment, the thickness varies in such a small range (± 10 nm) that it can be directly correlated to the change in reflectivity [14]. This way, we can acquire one single image in each of the four available LEDs at the beginning of the experiment, calculate the reflectance curve, and then use the resulting reflectance curve to create a look-up table for the conversion from reflectance to biomass thickness. The images were acquired with a simple CCD camera (PointGrey) and analyzed through a custom-made ImageJ plugin and a MATLAB software. More details about the conversion from reflectance values to mass density can be found elsewhere [7, 14].

### Chip surface functionalization

The experiments were performed on 25 × 12.5 mm silicon chips (Fig. S2a), purchased from Silicon Valley Microelectronics (Santa Clara, CA) with a 110-nm layer of silicon oxide grown on top. Chips were spotted with a SciFlexArrayer S12 spotter (Scenion, Berlin, Germany). For what concerns localized functionalization samples, polymer solutions were prepared by diluting them up to 0.014% in water with sucrose monolaurate 0.01% *w/v*. 400 pL of these solutions was spotted on untreated IRIS chips. Then, for the protein microarrays, 400 pL of either native or DBCO-modified α-Lactalbumin 1 mg/mL was spotted on top of that. Instead, for the peptide microarray, LAC-1 peptides were first dissolved in DMSO at a stock concentration of 1 mM. LAC-1 was then diluted in PBS at a concentration of 100 uM, while LAC-1-Prg was diluted at the same concentration into the printing buffer suitable for CuACC conjugation: 25 mM Na/Acetate p4.8, 15 mM trehalose, 100 mM CuSO4, 400 mM THPTA, and 6.25 mM ascorbic acid. 400 pL of peptide solutions obtained this way was finally deposited on top of polymer-spotted chips.

In both cases, the spotted chips were left overnight in a NaCl saturated humid chamber. The chips were washed with a 0.5% *w/v* water solution of a copolymer of dimethylacrylamide and allyl glycidyl ether (EPDMA) synthesized as reported elsewhere [15]. This polymer, originally developed to suppress electroosmotic flow in capillary electrophoresis, is known for its ability to form a thin layer on glassy surface with antifouling properties by dip and rinse approach.

Some experiments for this work were also performed in a flat coating configuration. For these experiments, the samples were prepared in a different way. Briefly, the surface of the chips was first oxygen plasma activated for 10 min, and then the chips were immersed in the aqueous polymer solutions (1%, *w/v* polymer in an aqueous solution of 20% saturated ammonium sulfate) for 30 min. Afterwards, the substrates were washed with DI water and dried under nitrogen stream. Finally, to complete the coating procedure, they were baked in a stove at 80 °C for 15 min. The chips were then spotted with 400 pL of native α-Lactalbumin 1 mg/mL. As above, the spotted chips were left overnight in a NaCl saturated humid chamber. In this case, a 1-h blocking step with a 50 mM ethanolamine solution was performed to inactivate the residual amine groups on the surface.

### Microfluidic chamber

Prior to starting the experiment, every chip (ESM Fig. S2a, S2b) was topped with an adhesive spacer and an AR coated glass slide to form a chamber for in-liquid measurements. The glass was purchased from Abrisa Technology (Torrance, CA) while the spacer was customized for us by Grace BioLabs (Bend, OR). The volume of the chamber obtained this way was less than 5 uL. The whole system has a dead volume of less than 500 uL.

## Results and discussion

### Localized surface functionalization: testing many surface chemistries on the same chip

The adhesive characteristics of DMA, MAPS copolymers allow to generate films on localized regions of the substrate by spotting pL amounts of polymer solutions. Two sets of polymers were used in this experiment: one contains succinimide esters while the second one contains azide groups. In each series, three variants were generated by copolymerizing, in addition to the backbone monomers, acrylic monomers bearing carboxyl or tertiary amine groups or a mixture of both monomers in such a ratio to define a precise isoelectric point. At the pH used for the hybridization, the surface is negatively or positively charged in the first two cases. The net charge of the amphoteric surface can be tuned from negative to positive depending on the pH of the hybridization buffer. In the experimental conditions used here, it has an overall negative charge. In addition, the charge can be modulated by tailoring the ratio of the two acrylamido buffers in the polymer or by selecting different acrylamido buffers pairs.

The parent polymers, Copoly NAS 10%, and its derivative Copoly Azide are neutral or only negligibly charged; they bind either native proteins by nucleophile reaction between succinimidyl esters and amino groups naturally present in proteins, or DBCO-modified proteins by azide-alkyne strain promoted cycloaddition, a classical click chemistry reaction [16, 17].

In Fig. 2a, a schematic representation of the functionalization is reported, compared to the classic flat

coating solution (Fig. 2b). In a single spotting section, aqueous solutions of ten polymers at 0.014% *w/v* were spotted in array format. On top of each polymer, the same protein, α-Lactalbumin (either native or DBCO-modified) at a concentration of 1 mg/mL, was deposited. To avoid non-specific adsorption of biomolecules on the area surrounding the spots, after deposition of the capture probe, a blocking step was performed using a hydrophilic polymer, EPDMA, previously reported by our group [15]. For what concerns non-specific binding to the polymers below the biomolecule spots, that is assumed to be very similar for all polymers, since they all possess the same backbone. Moreover, the low incidence of non-specific binding in this type of polymers (less than 4%) has been previously demonstrated by our group [18].

An IRIS image of the dry chip is displayed in Fig. 2c. Distinct groups of spots show different levels of brightness and therefore highlight a variability in mass density. The brighter spots are indeed a result of the better immobilization capacity of the polymer underneath.

The chip was used to run a 60-min long in-liquid IRIS experiment. First, filtered PBS buffer was flowed into the chamber for 15 min, allowing the system to stabilize. Afterwards, anti-α-Lactalbumin antibody at 1 μg/mL (≈ 7 nM) was injected for 20 min at an average speed of 200uL/min. PBS buffer was then injected as a washing buffer for another 20 min. Finally, the surface was restored by flowing a 100 mM glycine solution at pH = 2 for 5 min. During this whole experiment, interferometric images were acquired. To get a better signal-to-noise ratio, each image was the average of 100 acquired frames. Each point of the curve in Fig. 3 corresponds to one acquired image. To obtain the values displayed in Fig. 3 from the images, circle ROIs to enclose each spot were drawn in ImageJ, while a ring around every spot was taken as the background. The average signal of the ROIs was measured and the final differential values were obtained by subtracting from the mean value of each spot the mean value of its anular background. As it may be noticed in Fig. 2c, some of the spots are slightly inhomogeneous. However, our technique proposes to measure the average increase of mass per unit area on the whole spot area; therefore, the inhomogeneties were considered as part of the statistics and less homogeneous spots were not discarded.

By analyzing the first 20 min of data, as detailed in par. 2.2, the binding curves in Fig. 3a were obtained. A simple Langmuir one-to-one binding equation was used to fit the data (Eq. 1a).

$$\mathrm{dm}(t) = meq \cdot \frac{k_{ON}C}{k_{ON}C + k_{OFF}} \cdot \left(1 - e^{-(k_{ON}C + k_{OFF})\cdot t}\right) \tag{1a}$$

where *dm(t)* indicates the differential mass density, *t* is the time in seconds, $m_{eq}$ is the mass density value reached at the equilibrium, $k_{ON}$ is the association rate, $k_{OFF}$ is the dissociation rate, and *C* is the concentration of the analyte in solution, that, in our case, is around 7 nM.

The equilibrium dissociation constant ($K_D$) was found as follows:

$$K_D = \frac{k_{OFF}}{k_{ON}} = \frac{[R][L]}{[RL]} \tag{1b}$$

where [L] is the concentration of the analyte in solution (which in our case equals C), [R] is the concentration of the probe on the surface (that is, the number of the binding sites), and [RL] is the concentration of the compound.

This way, we could estimate the dynamic constants of the reactions. The parameters obtained from this analysis are

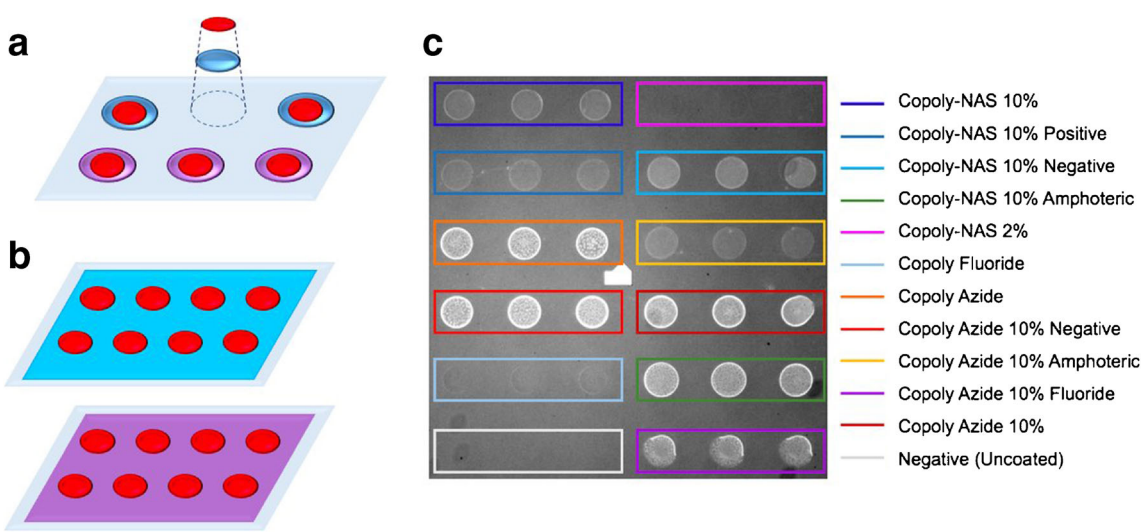


**Fig. 2** On the left, a simplified scheme of the spotted polymers technique (**a**) and flat coating technique (**b**). On the right, a dry IRIS chip image acquired before starting the real-time binding experiment. On the chip, a 6 × 6 matrix of α-Lactalbumin spots is visible. Each group of three spots corresponds to a different polymer (**c**)

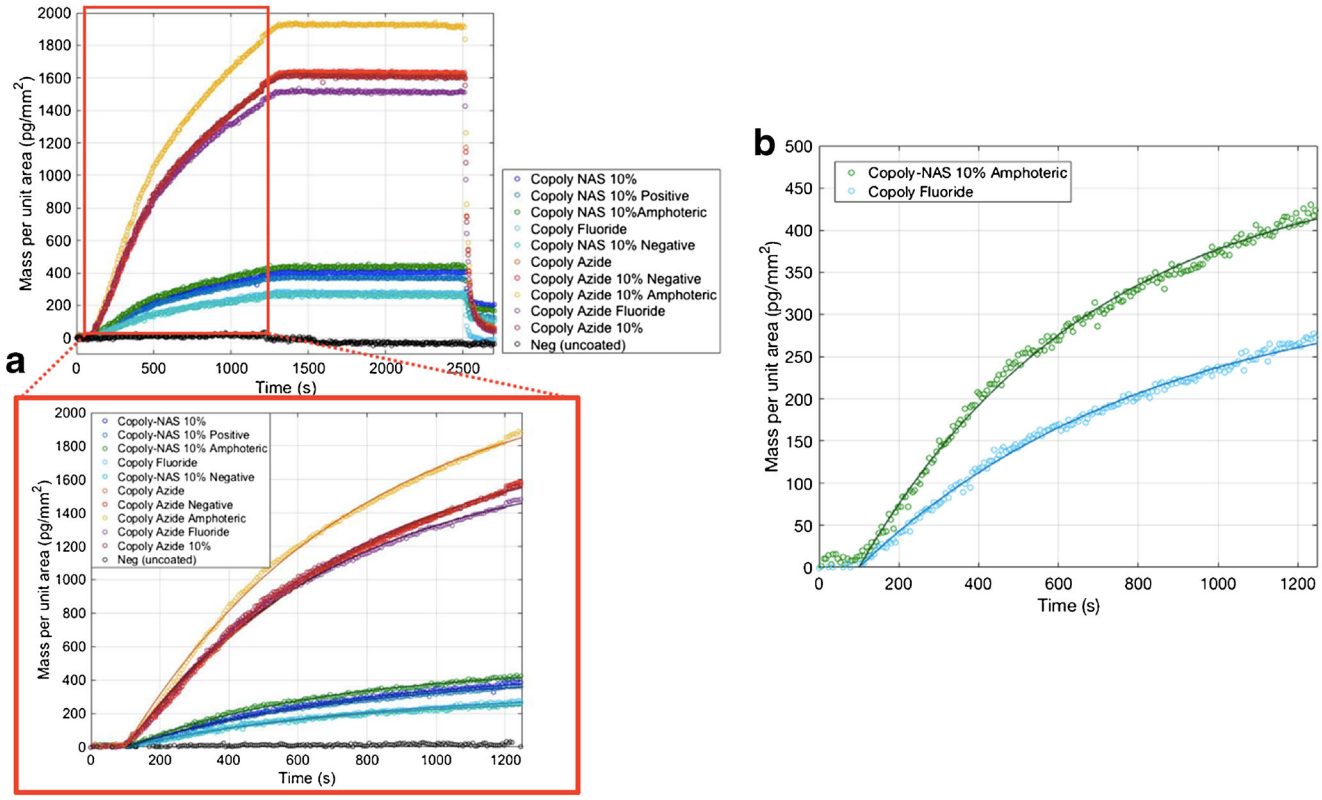


**Fig. 3** Anti-α-Lactalbumin binding to two different modifications of α-Lactalbumin spotted on a single IRIS chip. The solid lines in the inset (**a**) show a classic Langmuir fit of the data. The inset (**b**) focuses on Copoly Fluoride and Copoly-NAS 10% Amphoteric curves, the only two polymers that were also studied in a flat-coating configuration

reported in Table 2. Applying this one-to-one binding model might be seen as an oversimplification, but for our comparison purposes, the approximation holds, since the fitting results are satisfyingly good, with a $R^2$ factor that always exceeds 0.99.

As it can be noticed from Fig. 3, the two families of polymers are clearly distinct in terms of equilibrium points reached. However, the equilibrium constants that were calculated with the Langmuir model seem to suggest that the dynamic behavior of the antibody is similar in all cases (Table 2). As a matter of fact, the ON and OFF rate of all the polymer spots is in the same range. This suggests that, while it may be reasonable to think that the equilibrium point reached could depend on the concentration of the immobilized probe, the latter does not appear to influence the dynamic behavior of the antibody.

To further verify that, we considered the correlation between the equilibrium point reached by each curve and the average initial mass per spot. Table 3 lists the value of the initial mass on the surface for the different polymers. In this dataset, the row relative to the negative spot refers to the protein spotted on the untreated $Si/SiO_2$ surface with no polymer underneath. The mass value shown for this region is negative,

**Table 2** ON and OFF rates obtained through a classic Langmuir fit of anti-α-Lactalbumin binding on different α-Lactalbumin modifications, spotted on top of different polymers spots

| Copolymer | $k_{ON}$ ($10^4 M^{-1}s^{-1}$) | $k_{OFF}$ ($10^{-4}$ $s^{-1}$) | $K_D$ ($10^{-8}$ M) |
|---|---|---|---|
| Copoly NAS 10% | 9.4 ± 0.2 | 7.2 ± 0.1 | 0.77 ± 0.02 |
| Copoly NAS 10% positive | 9.0 ± 0.1 | 7.7 ± 0.3 | 0.86 ± 0.04 |
| Copoly NAS 10% negative | 8.3 ± 0.2 | 9.7 ± 0.6 | 1.17 ± 0.08 |
| Copoly NAS 10% amphoteric | 11.1 ± 0.2 | 6.5 ± 0.1 | 0.59 ± 0.01 |
| Copoly fluoride | 6.5 ± 0.1 | 8.8 ± 0.4 | 1.35 ± 0.07 |
| Copoly azide | 7.7 ± 0.1 | 8.4 ± 0.3 | 1.09 ± 0.04 |
| Copoly azide 10% negative | 7.5 ± 0.7 | 7.8 ± 0.2 | 1.04 ± 0.10 |
| Copoly azide 10% amphoteric | 9.6 ± 0.9 | 8.2 ± 0.3 | 0.85 ± 0.09 |
| Copoly azide 10% fluoride | 8.0 ± 0.8 | 9.0 ± 0.3 | 1.13 ± 0.12 |
| Copoly azide 10% | 9.8 ± 0.1 | 8.8 ± 0.2 | 1.00 ± 0.03 |

**Table 3** Initial mass density values for the α-Lactalbumin spots on different polymers

| Copolymer | Initial mass density (ng/mm$^2$) |
|---|---|
| Copoly NAS 10% | 1.36 ± 0.02 |
| Copoly NAS 10% positive | 0.66 ± 0.02 |
| Copoly NAS 10%negative | 1.17 ± 0.03 |
| Copoly NAS 10% amphoteric | 1.09 ± 0.06 |
| Copoly fluoride | 0.73 ± 0.04 |
| Copoly azide | 1.69 ± 0.07 |
| Copoly azide 10% negative | 3.92 ± 0.03 |
| Copoly azide 10% amphoteric | 3.83 ± 0.04 |
| Copoly azide 10% fluoride | 2.89 ± 0.04 |
| Copoly azide 10% | 1.93 ± 0.03 |
| Negative (uncoated) | −0.69 ± 0.05 |

which means that the background region around the spot is "taller" (or "thicker") than the spot itself. This may be explained by considering the blocking step we performed to passivize the surface before the experiment. Indeed, the neutral polymer solution we used to inactivate the surface is optimized to not bind to biomolecules. Since the blocking step is performed after spotting, with no washing in between, the neutral polymer forms a thin layer on the surface except for the spotted regions. When the chip is washed, the molecules that were deposited on the bare surface are washed away, while the polymer stays there. This leaves a "hole" where the spots used to be. Therefore, the differential value of the mass density results to be negative.

To quantitatively evaluate the correlation between the mass of the immobilized probe and the final mass of the compound, we calculated the Pearson's correlation coefficient (PCC) [19] between the two variables, as in Eq. 3.

$$\rho_{m_0,m_{eq}} = \frac{cov(m_0, m_{eq})}{\sigma_{m_0} \cdot \sigma_{m_{eq}}} \tag{3}$$

This calculation led to a correlation coefficient value of 0.85, which can be considered significant for our purposes (ESM Fig. S3). Here, a positive correlation does not necessarily involve a linear correlation, which was indeed not expected, since the correlation pattern in this case is complicated and many parameters must be considered. However, a positive PCC accounts for the fact that having a larger number of immobilized molecules on the surface can lead to stronger binding. This is somewhat intuitive: increasing the number of immobilized molecules means increasing the concentration of binding sites on the surface ([R] in Eq. 1a), which in turn allows more analyte molecules ([L] in Eq. 1b) to bind, leading to a higher final concentration of the compound ([LR] in Eq. 1b). However, since we are primarily interested in determining the reactivity of the molecules, a good approach would be to normalize the curves above by dividing them for the initial mass value (Fig. 4). This way, we can estimate how reactive the molecules are per unit of probe concentration.

This normalization shows that having a large quantity of biomaterial immobilized on the surface is not always a good indication of the high reactivity of the probes. As an example, even if the overall binding is higher on the Copoly Azide 10% amphoteric spot (Fig. 3a), in the end, the neutral Copoly Azide spot almost doubles its mass density ($m/m_0 \approx 1$, orange curve in Fig. 4), while the former accumulates less than half of the initial mass value ($m/m_0 \approx 0.5$, yellow curve in Fig. 4). A possible explanation for this is that the presence of charges could inhibit the binding of this specific antibody due to electrostatic repulsion. Another possibility is that the charged polymers immobilize the probe so tightly that they modify its structure and therefore affect its reactivity. This second possibility is less probable, since α-Lactalbumin is quite symmetric and the charges are well distributed on its surface.

To summarize, even though the neutral polymers retain less mass from spotting (Table 2, Fig. 3), the molecules that are immobilized onto those seem to demonstrate a higher reactivity (Fig. 4). Actually, concluding this with absolute certainty would only be possible if we could provide a dataset where each polymer had the same identical initial mass value. However,

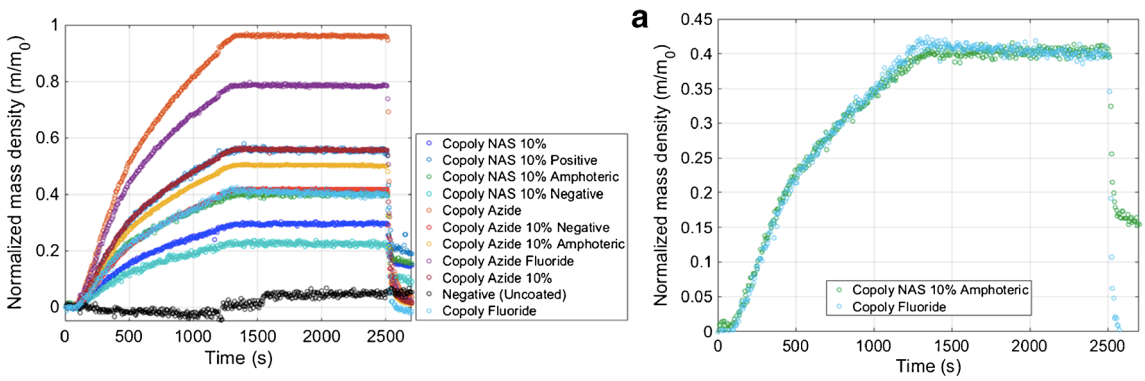


**Fig. 4** The curves in Fig. 3a, normalized by dividing every curve for the initial mass value. The inset (**a**) focuses on the two polymers that were also tested in a flat coating configuration

this is impossible to obtain, since the amount of biomass that is adsorbed onto the surface through the spotting procedure is a factor we cannot control. Therefore, normalizing for it gives us the best possible estimate of the reactivity of the probes.

### Comparison to flat coating

To further demonstrate that our assay is comparable to the classical flat coating method, in terms of qualitative performance of the polymers, we chose two of the polymers mentioned above, namely Copoly NAS 10% amphoteric and Copoly Fluoride, and we performed the same measurements in a flat coating configuration.

First, two chips were coated with, respectively, Copoly Fluoride and Copoly NAS 10% amphoteric, with the classical flat coating procedure as described in the "Material and Methods" section (Par. 2.3).

On both chips, the same IRIS experiment described above was performed: the chamber was mounted, with the glass and spacer, and the obtained cartridge was positioned inside the instrument. PBS buffer was flowed into the chamber for 15 min to stabilize the system. Afterwards, anti-α-Lactalbumin 1 μg/mL (≈ 7 nM) was injected and recirculated for 20 min at an average speed of 200 uL/min. A 20-min washing with PBS was performed, and a 5-min surface restoration with a 100 mM glycine solution (pH = 2) was used to go back to the starting point.

As for the experiment described in Paragraph 3.1, every point of the curves displayed in Fig. 5 corresponds to the average of 100 acquired frames.

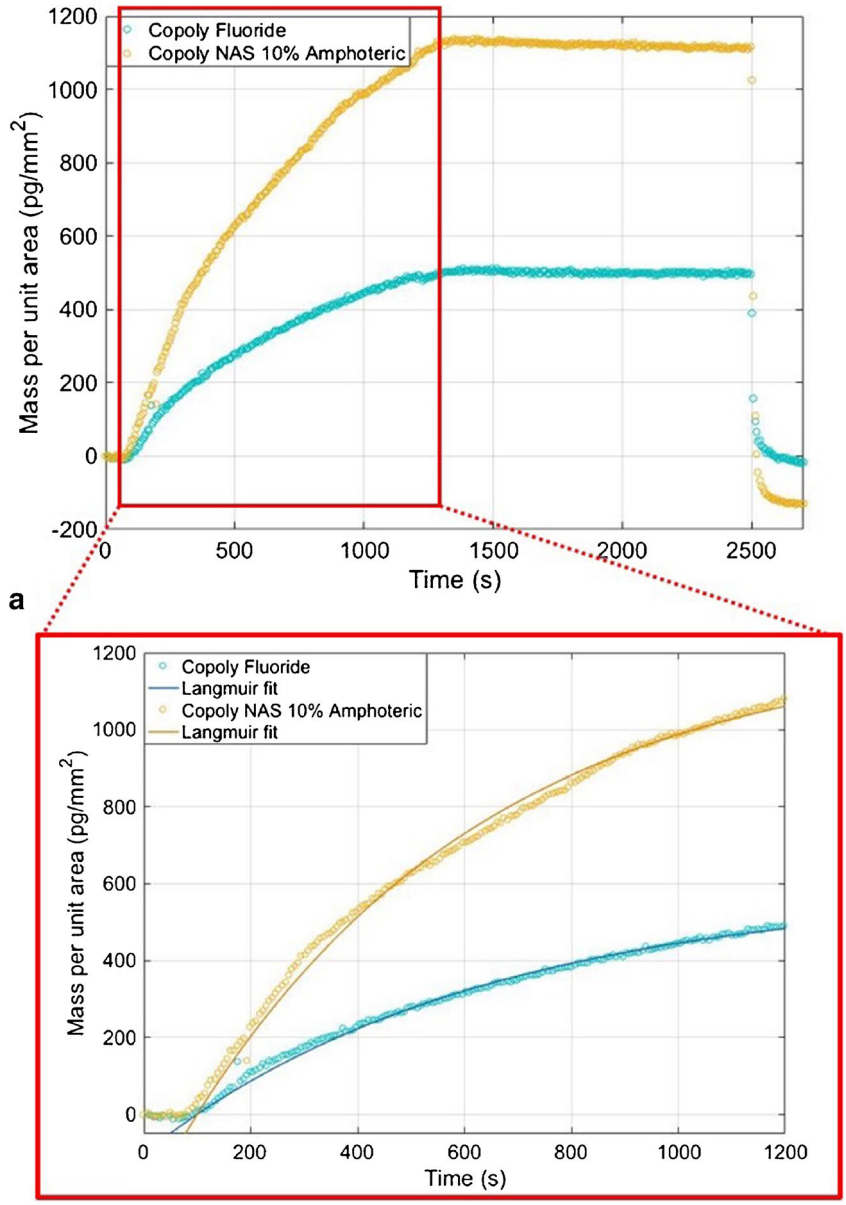


**Fig. 5** Anti-α-Lactalbumin binding to α-Lactalbumin spotted on two flat-coated IRIS chips: one coated with Copoly Fluoride (light blue curve) and one with Copoly NAS 10% Amphoteric (yellow). The solid lines in the inset (a) show a classic Langmuir fit of the data

The dynamical parameters relative to the curves shown in Fig. 5 can be found in Table S2 (see ESM). By comparing Figs. 3b and 5, one can notice that in both cases, the equilibrium point reached by the Copoly Fluoride curve is sensibly lower than the one reached by Copoly NAS 10% amphoteric.

Moreover, the initial mass values can be compared in the two cases (ESM Table S3), and it can be observed that they are similar. A perfect agreement was indeed not expected, since the percentage of polymer used is quite different.

To investigate the problem in depth, we normalized these data the same way we did above, by dividing the curves for the initial mass value (ESM Fig. S4). The result confirmed the previous findings: the two polymers behave the same way in terms of reactivity, as it also emerges from the data in Fig. 4a, where the Copoly Fluoride curve is following the same path as the Copoly NAS 10% amphoteric one.

### Localized immobilization of LAC-1 peptide

In order to further demonstrate the power of the localized functionalization method, we applied it to the immobilization and functional test of a model peptide, LAC-1, which is an epitope belonging to the N-terminal part of α-Lactalbumin protein. This epitope is the most reactive of the characterized series [20] and was synthesized in two modifications, as described in the "Material and Methods" section (Par. 2.4).

We have previously shown that the chemistry used to immobilize peptides has a crucial role on their reactivity [21] by demonstrating that immobilization of a collection of peptides on NAS copolymers resulted in a loss of reactivity of the probes when the microarray was incubated with human serum from cystic fibrosis (CF) patients affected by *Burkholderia* infections. On the other hand, when the same peptides were immobilized on Copoly Azide through a click chemistry reaction, their binding affinity towards serum antibodies was enhanced providing discrimination between healthy and affected individuals in a serological assay for *Burkholderia*. Therefore, peptides are good candidates for our method to show the difference that surface chemistry can make on the reactivity of biomolecules. Focusing on the model peptide chosen here, we also showed that the reactivity of LAC-1 in fluorescence measurements is crucially related to the spacing between the probes, its availability to bind being diminished by overcrowding effects [12].

We spotted an IRIS chip according to the protocol described in the "Material and Methods" section (Par. 2.6). In Fig. S5 (see ESM), an image of the dry IRIS chip can be observed. One can notice that LAC-1 spots on different polymers, diversely from α-Lactalbumin ones (Fig. 2c), look almost uniformly bright. This is an indication of the fact that the initial mass on all the spots is similar (ESM Table S4).

We performed IRIS real-time measurements on this chip to detect the binding of anti-α-Lactalbumin antibody. The experiment was carried out in an identical manner as the one described in Par. 3.1., except for antibody concentration, which was higher: 5 μg/mL (≈ 35 nM). The peptide has indeed a lower binding affinity to the antibody with respect to the protein [20].

By analyzing the images acquired through the IRIS setup, as already described in Par. 3.1, we obtained the binding curves displayed in Fig. 6a. Noticeably, not much difference is observable between the curves. However, when normalizing for the initial mass value (Fig. 6b), Copoly Azide curve stands out. This corroborates our previous findings that Copoly Azide is the most suitable polymer for maintaining a high reactivity of the peptide, while immobilizing an adequate quantity [21]. Moreover, having a higher concentration of the Azide copolymer on the surface does not seem to increase binding affinity; instead, it decreases it. This could be due to overcrowding effects, as we previously hypothesized [12], where we related the spacing between probes on the surface with their reactivity.

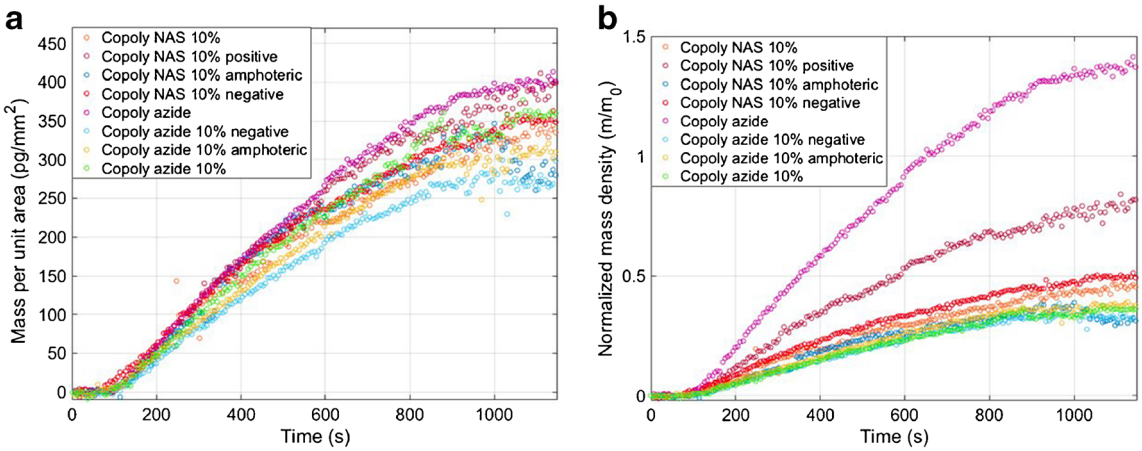


**Fig. 6** Application of the localized functionalization method to the immobilization of LAC-1 peptide. **a** Anti-α-Lactalbumin binding to two different modifications of LAC-1 spotted on a single IRIS chip. Each curve corresponds to a different spotted polymer. **b** The curves in Fig. 6a, normalized by dividing each of them by the initial mass density value

The calculation of the correlation between the initial mass density value and the equilibrium point reached by the curves (Eq. 2) yielded a negative value for the correlation coefficient ($\rho = -0.59$), indicating that, in this specific case, the immobilization capacity of the polymers is uncorrelated with the reactivity of the probes (ESM Fig. S6).

Interestingly, the charged Azide copolymers behave similarly to the NAS ones; this could be related to the negative overall charge that they assume in these conditions, which could inhibit binding due to electrostatic repulsion. This hypothesis is also validated by the fact that the positively charged 10% NAS copolymer has an increased reactivity with respect to the other members of the same family.

## Conclusions

In summary, we pursued the effort started in our latest work [6] of developing an innovative assay that allows to simultaneously test the performance of different surface chemistries, localized on distinct regions of the same support. Most importantly, we demonstrated that this immobilization technology can successfully be applied to proteins, as well as oligonucleotides, which is not trivial and could be challenging due to the complexity of protein structure. Briefly, we precisely quantified both the initial mass immobilized on each localized polymer spot as well as the final yield of the reaction. Moreover, we calculated the correlation between those values and, thanks to the real-time binding measurements, we could estimate the actual reactivity of the probes by applying a simple normalization. Single 60-min experiments were therefore enough to collect all the information that is necessary to qualitatively compare the performance of the different polymers. The results were in optimal agreement with those obtained in the classical flat coating configuration. We therefore showed that the combination of this localized functionalization technology and the real-time, in-liquid IRIS technique allows the user to quickly understand which surface chemistry would better suit any specific application. Furthermore, it removes the limitation regarding the number of molecules with different chemistries that can be immobilized on the same support.

**Funding information** This work was partially funded by Regione Lombardia, project AMANDA (Abnormal Metabolic states, cellular stressors and NeuroDegenerative processes).

## Compliance with ethical standards

**Conflict of interest** The authors declare that they have no conflict of interest.

All authors have participated in conception and design, or analysis and interpretation of the data; drafting the article or revising it critically for important intellectual content; and approval of the final version. This manuscript has not been submitted to, nor is under review at, another journal or publishing venue.

## References

1. MacBeath G. Protein microarrays and proteomics. Nat Genet. 2002;32(Suppl):526–32. https://doi.org/10.1038/ng1037.
2. Schena M, Shalon D, Davis RW, Brown PO. Quantitative monitoring of gene expression patterns with a complementary DNA microarray. Science. 1995;270:467–70. https://doi.org/10.1126/science.270.5235.467.
3. Pirri G, Damin F, Chiari M, Bontempi E, Depero LE. Characterization of a polymeric adsorbed coating for DNA microarray glass slides. Anal Chem. 2004;76:1352–8. https://doi.org/10.1021/ac0352629.
4. Sola L, Damin F, Gagni P, Consonni R, Chiari M. Synthesis of clickable coating polymers by post-polymerization modification: application in microarray technology. Langmuir. 2016;32:10284–95. https://doi.org/10.1021/acs.langmuir.6b02816.
5. Zilio C, Sola L, Damin F, Faggioni L, Chiari M. Universal hydrophilic coating of thermoplastic polymers currently used in microfluidics. Biomed Microdevices. 2014;16:107–14. https://doi.org/10.1007/s10544-013-9810-8.
6. Sola L, Damin F, Chiari M. Array of multifunctional polymers for localized immobilization of biomolecules on microarray substrates. Anal Chim Acta. 2019;1047:188–96. https://doi.org/10.1016/j.aca.2018.10.006.
7. Daaboul GG, Vedula RS, Ahn S, Lopez CA, Reddington A, Ozkumur E, et al. LED-based interferometric reflectance imaging sensor for quantitative dynamic monitoring of biomolecular interactions. Biosens Bioelectron. 2011;26:2221–7. https://doi.org/10.1016/j.bios.2010.09.038.
8. Mammen M, Dahmann G, Whitesides GM. Effective inhibitors of hemagglutination by influenza virus synthesized from polymers having active ester groups. Insight into mechanism of inhibition. J Med Chem. 1995;38:4179–90. https://doi.org/10.1021/jm00021a007.
9. Landi F, Johansson CM, Campopiano DJ, Hulme AN. Synthesis and application of a new cleavable linker for "click"-based affinity chromatography. Org Biomol Chem. 2010;8:56–9. https://doi.org/10.1039/b916693a.
10. Sola L, Chiari M. Modulation of electroosmotic flow in capillary electrophoresis using functional polymer coatings. J Chromatogr A. 2012;1270:324–9. https://doi.org/10.1016/j.chroma.2012.10.039.
11. Sola L, Damin F, Cretich M, Chiari M. Novel polymeric coatings with tailored hydrophobicity to control spot size and morphology in DNA microarray. Sensors Actuators B Chem. 2016;231:412–22. https://doi.org/10.1016/j.snb.2016.03.049.
12. Gori A, Cretich M, Vanna R, Sola L, Gagni P, Bruni G, et al. Multiple epitope presentation and surface density control enabled by chemoselective immobilization lead to enhanced performance in IgE-binding fingerprinting on peptide microarrays. Anal Chim Acta. 2017;983:189–97. https://doi.org/10.1016/j.aca.2017.06.027.
13. Needham J, Lortlar Ünlü N, Ünlü MS. Interferometric reflectance imaging sensor (IRIS) for molecular kinetics with a low-cost, disposable fluidic cartridge. In: Fitzgerald J, Fenniri H, editors. Biomimetic sensing. Methods in Molecular Biology, volume 2027. New York, NY: Humana; 2019. p. 15–28.
14. Sevenler D, Ünlü MS. Numerical techniques for high-throughput reflectance interference biosensing. J Mod Opt. 2016;63:1115–20. https://doi.org/10.1080/09500340.2015.1117668.
15. Chiari M, Cretich M, Damin F, Ceriotti L, Consonni R. New adsorbed coatings for capillary electrophoresis. Electrophoresis. 2000;21:909–16. https://doi.org/10.1002/(SICI)1522-2683(20000301)21:5<909::AID-ELPS909>3.0.CO;2-L.
16. Dommerholt J, Rutjes FPJT, van Delft FL. Strain-promoted 1,3-dipolar cycloaddition of cycloalkynes and organic azides. Top Curr Chem (Z). 2016;374:16. doi:10.1007/s41061-016-0016-4

17. Singh S, Dubinsky-Davidchika IS, Kluger R. Strain-promoted azide–alkyne cycloaddition for protein–protein coupling in the formation of a bis-hemoglobin as a copper-free oxygen carrier. Org Biomol Chem. 2016;14:10011–7. https://doi.org/10.1039/C6OB01817C.
18. Platt GW, Damin F, Swann MJ, Metton I, Skorski G, Cretich M, et al. Allergen immobilisation and signal amplification by quantum dots for use in a biosensor assay of IgE in serum. Biosens Bioelectron. 2014;52:82–8. https://doi.org/10.1016/j.bios.2013.08.019.
19. Pearson's Correlation Coefficient. In: Encyclopedia of Public Health. Kirch W, editor. Springer, Dordrecht; 2008. doi:10.1007/978-1-4020-5614-7
20. Hochwallner H, Schulmeister U, Swoboda I, Focke-Tejkl M, Civaj V, Balic N, et al. Visualization of clustered IgE epitopes on α-lactalbumin. J Allergy Clin Immunol. 2010;125. https://doi.org/10.1016/j.jaci.2010.03.007.
21. Gori A, Sola L, Gagni P, Bruni G, Liprino M, Peri C, et al. Screening complex biological samples with peptide microarrays: the favorable impact of probe orientation via chemoselective immobilization strategies on clickable polymeric coatings. Bioconjug Chem. 2016;27:2669–77. https://doi.org/10.1021/acs.bioconjchem.6b00426.

**Publisher's note** Springer Nature remains neutral with regard to jurisdictional claims in published maps and institutional affiliations.

**Analytical and Bioanalytical Chemistry**

**Electronic Supplementary Material**

# Simultaneous evaluation of multiple microarray surface chemistries through real-time interferometric imaging

Elisa Chiodi, Laura Sola, Dario Brambilla, Marina Cretich, Allison Marie Marn, M. Selim Ünlü, Marcella Chiari

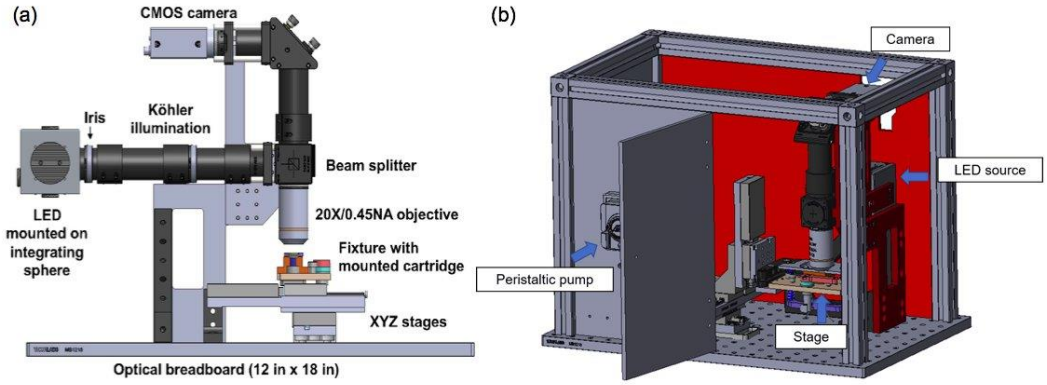


**Fig. S1** The IRIS setup: (a) optical scheme and (b) physical benchtop setup

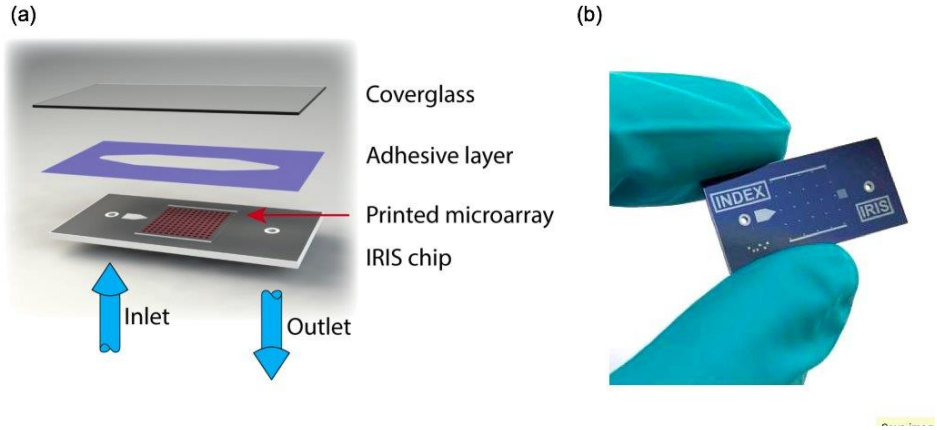


**Fig. S2** A scheme of the microfluidic chamber used for IRIS measurements (a) and an IRIS Si/$SiO_2$ chip (b)

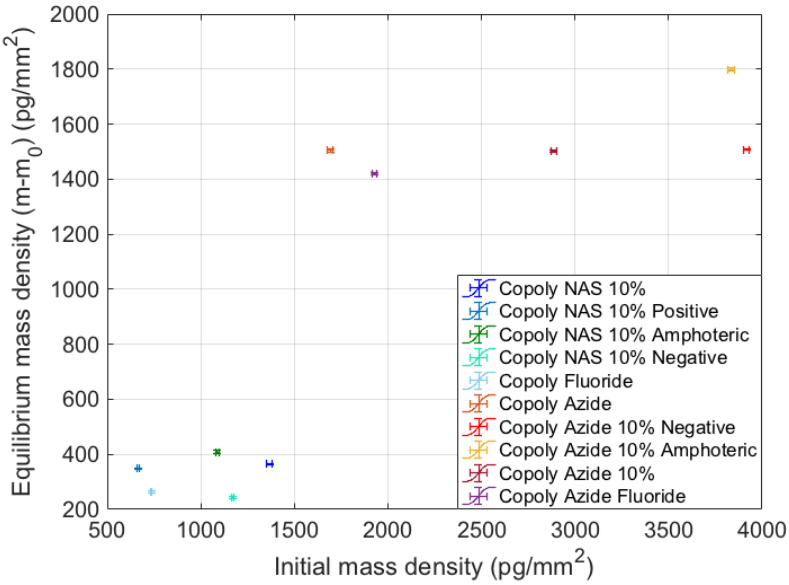


**Fig. S3** Correlation between the initial mass density value and the equilibrium value reached by the antibody binding to different polymer spots. The values are well correlated, with a value of the correlation coefficient $\rho = 0.85$

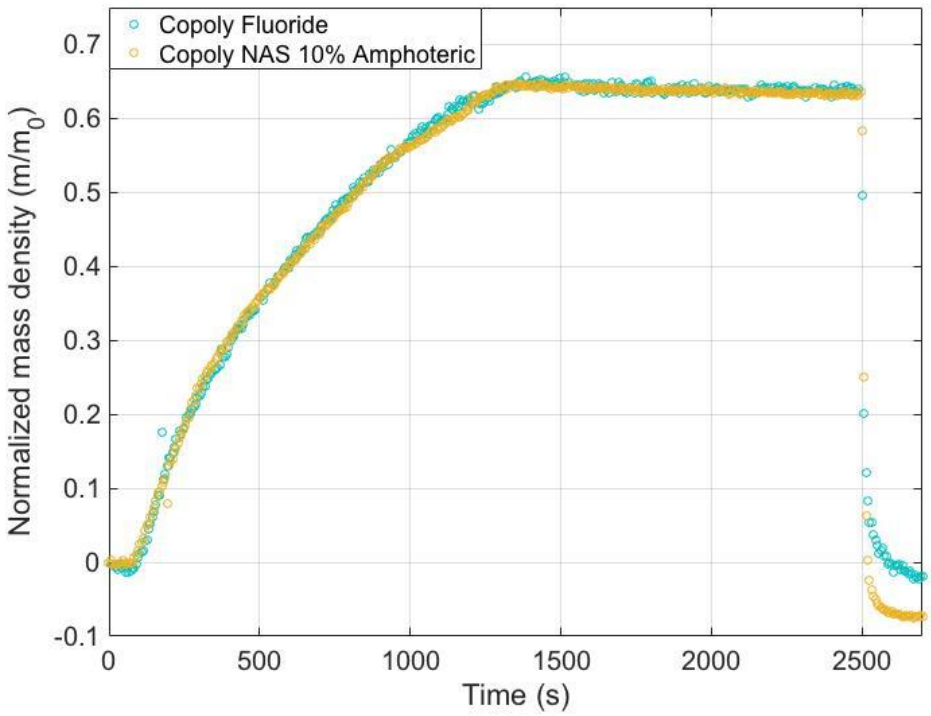


**Fig. S4** The curves in Figure 10, normalized by dividing each of them by the initial mass density value

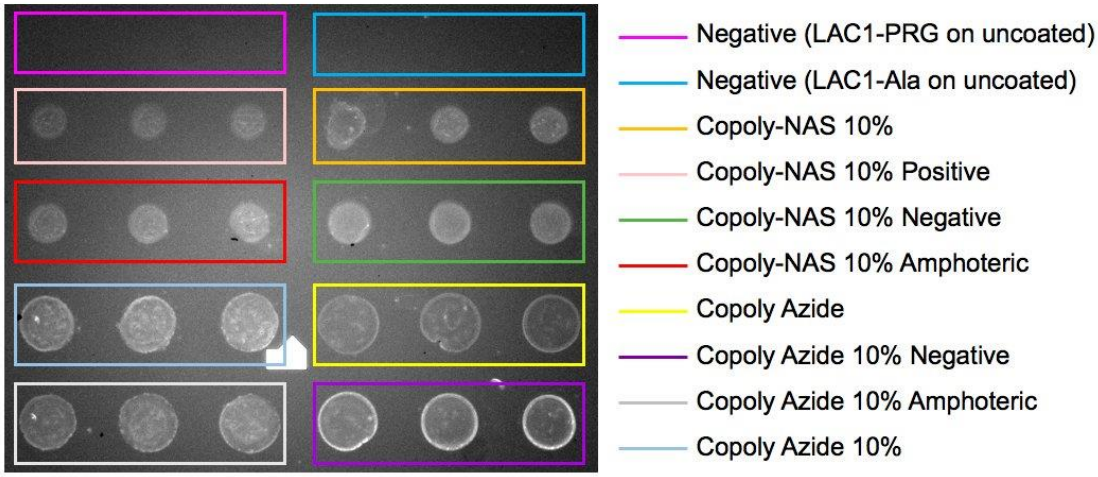


**Fig. S5** Dry IRIS chip image of the LAC-1 spotted chip acquired before starting the real-time binding experiment. On the chip a 6x6 matrix of LAC-1 spots is visible. Each group of three spots corresponds to a different polymer, as detailed in the legend

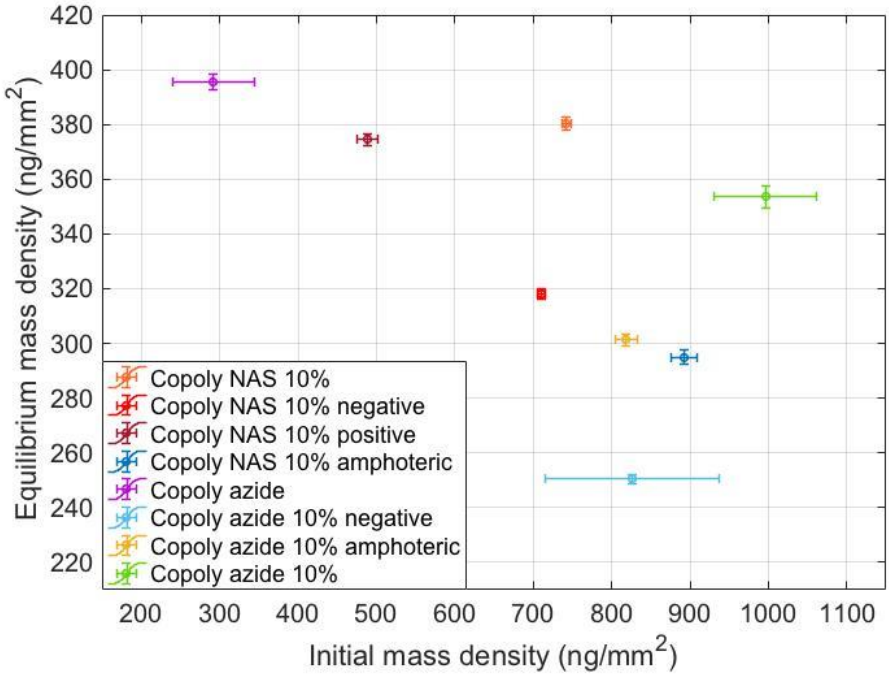


**Fig. S6** Correlation between the initial mass density value and the equilibrium value reached by the antibody binding to different LAC-1 peptide spots on different polymers. The values are not correlated, yielding a negative correlation coefficient ($\rho$ = -0.59)

**Table S1** Peptide sequences

| Peptide code | Sequence |
|---|---|
| **LAC1** | EQLTKAEVFRELKDLKGYG |
| **LAC1-Prg** | EQLTKAEVFRELKDLKGYG-Prg |

**Table S2** ON and OFF rates obtained through a classic Langmuir fit of anti- $\alpha$-lactalbumin binding on spotted Copoly Fluoride (blue curve, fig.4a) and on spotted Copoly NAS 10% amphoteric (yellow curve, fig.4a)

| Copolymer | $k_{ON}$ ($10^4 M^{-1}s^{-1}$) | $k_{OFF}$($10^{-4}s^{-1}$) | $K_D$($10^{-8}M$) |
|---|---|---|---|
| **Copoly Fluoride** | 1.4 ± 0.1 | 15.9 ± 0.4 | 11.6 ± 0.4 |
| **Copoly NAS 10% amphoteric** | 3.0 ± 0.1 | 14.4 ± 0.4 | 4.8 ± 0.2 |

**Table S3** Comparison of the initial mass density value for Copoly Fluoride and Copoly NAS 10% amphoteric polymers for the two experiments

| Copolymer | Spotted initial mass density ($ng/mm^2$) | Flat-coated initial mass density ($ng/mm^2$) |
|---|---|---|
| **Copoly NAS 10% amphoteric** | 1.09 ± 0.06 | 1.76± 0.02 |
| **Copoly Fluoride** | 0.73 ± 0.04 | 0.78± 0.01 |

**Table S4** Initial mass density values for the LAC-1 spots on different polymers

| Copolymer | Initial mass density ($ng/mm^2$) |
|---|---|
| **Copoly NAS 10%** | 0.74 ± 0.02 |
| **Copoly NAS 10% positive** | 0.49 ± 0.02 |
| **Copoly NAS 10% negative** | 0.71 ± 0.02 |
| **Copoly NAS 10% amphoteric** | 0.89 ± 0.03 |
| **Copoly Azide** | 0.39 ± 0.05 |
| **Copoly Azide 10% negative** | 0.87 ± 0.10 |
| **Copoly Azide 10% amphoteric** | 0.81 ± 0.02 |
| **Copoly Azide 10%** | 1.00 ± 0.08 |
| **Negative (LAC-1 on uncoated)** | -0.38 ± 0.02 |
| **Negative (LAC-1 PRG on uncoated)** | -0.35 ± 0.02 |

**Table S5** ON and OFF rates obtained through a classic Langmuir fit of anti- α-lactalbumin binding on different LAC-1 modifications*, spotted on top of distinct polymers spots

| **Copolymer** | **$k_{ON}$ ($10^4 M^{-1}s^{-1}$)** | **$k_{OFF}$ ($10^{-4}s^{-1}$)** | **$K_D$ ($10^{-8}M$)** |
|---|---|---|---|
| **Copoly NAS 10%** | 2.9 ± 0.1 | 3.0 ± 0.1 | 1.03 ± 0.05 |
| **Copoly NAS 10% positive** | 3.2 ± 0.1 | 1.2 ± 0.2 | 0.38 ± 0.06 |
| **Copoly NAS 10% negative** | 3.1 ± 0.1 | 2.9 ± 0.3 | 0.94 ± 0.10 |
| **Copoly NAS 10% amphoteric** | 3.0 ± 0.1 | 2.4 ± 0.1 | 0.80 ± 0.04 |
| **Copoly Azide** | 3.4 ± 0.1 | 0.4 ± 0.2 | 1.18 ± 0.06 |
| **Copoly Azide 10% negative** | 2.5 ± 0.2 | 4.6 ± 0.1 | 1.84 ± 0.15 |
| **Copoly Azide 10% amphoteric** | 2.7 ± 0.1 | 3.5 ± 0.1 | 1.30 ± 0.06 |
| **Copoly Azide 10%** | 2.9 ± 0.1 | 1.0 ± 0.5 | 0.35 ± 0.17 |

* There are actually two different modifications of LAC-1 on the surface, as detailed in Table S1.